CO-REGISTRATION OF LIDAR AND PHOTOGRAMMETRIC DATA FOR UPDATING BUILDING DATABASES

Costas Armenakis, Yu Gao, Gunho Sohn

Geomatics Engineering, GeoICT Lab
Department of Earth and Space Science and Engineering
York University, Toronto, Ontario, Canada
{armenc}{yugao86}{gsohn}@yorku.ca

Commission IV, IC WG IV/VIII

KEY WORDS: Lidar, photogrammetry, registration, planes, urban.

ABSTRACT:

Three dimensional data are required for the modeling of urban environments and determining their spatio-temporal changes. The required data are mainly acquired using photogrammetric and lidar collection methods and the data are collected either simultaneously or at different time epochs. In this paper we present the approach and the preliminary results of co-registering these two types of data. This data alignment is based on the 3D surface transformation, where the lidar point cloud is transformed in to the DSM reference system, thus permitting the accurate transformation of lidar data in the image space for determining any spatial changes. The transformation parameters are determined based on corresponding planar surfaces extracted in each data set. A region growing algorithm based on the normal vector directions of the generated TIN data is applied to extract planar clusters following by plane fitting to derive the plane primitives. The rotation and translation parameters between the DSM and lidar data are them determined based on the plane normal vectors and plane centroids. The transformed lidar point cloud is t then back-projected on the images used to derive the DSM and their image location serve to assess the quality of the co-registration.

1. INTRODUCTION

Nowadays, 3D building databases are used extensively in numerous applications such as 3D urban change detection, city planning and environmental assessment. In many occasions data from various sources are complimentary due to their inherent semantic and accuracy properties. Building databases are generated by various data sources but mainly aerial and satellite images and airborne laser scanning data are the most common ones. In several occasions these data are augmented by terrestrial images and lidar data as well, while in many occasions the data collection times are different as well.

Therefore, there is a need for the integration of the various heterogeneous datasets produced by different sensors and collected in different epochs. For this data conflation process it is essential that the multiple data sets are co-registered, the correspondence among the features is established, and the transformation function mapping one data set to the other is defined. Initially the space of co-registration is determined followed by the characterization of the invariant corresponding features to be matched between two or more data sets.

In our case we are interested in integrating photogrammetric and lidar data. The space of comparison was based on the minimum processing of the data sets. Lidar sensors provide a highly dense and accurate 3D irregular point cloud of the surveyed area. On the other hand optical sensors can produce relatively rapidly a photogrammetric digital surface model – regular or irregular- of the area of interest. Thus, the framework for the comparison is based on two 3D point sets covering the same area. However, there is no one-to-one point correspondence between the photogrammetric and lidar point-based 3D surfaces. In addition the 3D point data although cover the same area are referenced to the coordinate systems defined by their acquired sensors. Thus, even in the case of corresponding features their 3D positions will not coincide. The mapping function between the two can be very well based on the well known 3D conformal transformation, which establishes the relationship between two orthogonal reference systems. The critical issue here is to identify common features between the two 3D point data sets that will allow the determination of the parameters of the 3D conformal transformation.

Traditionally comparison of DSM data is based on establishing the point correspondence by establishing a common X,Y grid and derived the Z values of each DSM by interpolation. This allows for the estimation of the displacements between the two data sets but obviously is error prone to the interpolation, particular in urban areas. Another approach used for deriving the alignment between two point clouds is the Iterative Closest Point (ICP) method (Besl and Mckay, 1992). It is an iterative procedure requiring initial values and it is based on the minimization of the distance between a point belonging to one data set and its closest points in the second data set. No direct point correspondence, blunders and the large number of points are expected to affect the performance of the ICP algorithm in urban areas, although this needs to be confirmed by further testing.

Considering the urban environment and the 3D building modeling applications we observe that linear features and planar surfaces are important invariant geometric and semantic elements. This can lead to robust registration between the two data sets. Habib et al., 2004 used straight lines as the registration primitives, while planes for surface matching have been also used (Habib and Schenk, 1999; Schenk and Chatho, 2002; Sampath and Shan, 2006, Dold and Brenner, 2004). The quality of the integration outcomes unquestionably depends on

the oo-Registration process towards respective data (Postolov et al., 1999).

In our case of aligning lidar to photogrammetric data we initially investigate the use planar surfaces as the co-registration primitives as planar roofs are quite common feature in urban areas and planar features are more complete and contain greater thematic information than linear features.

2. METHODOLOGY

The proposed methodology is based on rigid 3D surface registration. Thus, it requires the definition and identification of common primitives between the two data sets followed by establishing the mapping parameters from one system to the other. The primitive features adopted in this work are planar patches. The approach is implemented by the following basic steps

1) Establishment of reference system.

2) Extraction of planar surfaces from both the photogrammetric and lidar data using region seed and region grown procedures.

3) Derivation of roof planes through plane fitting process.

4) Establishment of the correspondence between the photogrammetric and lidar planes.

5) Determination of the transformation parameters.

6) Assessment of the goodness of the co-registration process.

2.1 Reference system

Both data sets were acquired with sensor systems whose positions and orientations were derived based on GPS and IMU measurements, and therefore their object X, Y, Z coordinates were to the sensor coordinate system. All three coordinates were reduced to a common centroid coordinate system located in the study area. This was done to avoid any numerical instability in the solutions due to the very large numbers involved in the operations, especially when X and Y coordinates are in the UTM projection system.

2.2 Extraction of planar patches

Planar patches were extracted for both photogrammetric DSM and lidar data sets. The extraction process was based on a seeded region growing segmentation. Initially a Triangulation Irregular Network (TIN) was generated from the point data. Then a region growing segmentation was applied on the organized TIN data.

The implementation of region growing algorithm was based on initially selecting a seed (a triangle in our case) and compares its normal vector orientation to that of its neighbourhood to see if the neighbour triangle belongs to the same region as the seed. If the difference in the orientation of the normal vectors is smaller than the set threshold, then the neighbour triangle is included in the region and is labelled as belonging to this region planar cluster. After searching the entire neighbourhood of the current seed, the next element in the cluster list will be set as the new seed and the search is repeated in the new neighbourhood until all the elements in the region are processed. A new cluster will begin by searching for seed which will be the first triangle that has not been labelled as processed. Each cluster that passed the planarity test is now taken into the connected components analysis. The normal vector of each cluster is calculated and is used as the index of defining if neighbouring sub-planes lie on the same plane. An efficient metric for co-planarity considers the distance between neighbouring sub-planes (Chikomo et al., 2007). Clusters with close edges and similar orientation are then merged into consistent cluster.

2.3 Plane derivation

The plane parameters for each planar cluster were determined using a local plane fitting algorithm to each derive planar patches. The plane equation used was

$$Z = aX + bY + c$$

The plane parameters a, b, c were estimated by least squares adjustments by minimizing the sum of the squared residuals *v*. The outcome of the plane fitting are planes represented by their normal vectors $\vec{n}$ and centroid centers $\vec{m}$.

2.4 Plane correspondence

At this initial stage of the work the localization and matching of the conjugate common planes between photogrammetric and lidar data was perform manually. At this preliminary stage of the work three planes were initially selected from each data set.

2.5 Transformation parameters

A 3D conformal transformation is applied to establish the relationship of the two 3D point clouds. It consists of a 3D rotation matrix *R* and a 3D translation *T*. The scale factor is assumed to be equal to unit based on a rigid body motion and the fact that the two data sets are supposed to be absolutely oriented to the ground reference system.

The transformation parameters are estimated in two steps. Initially the rotation matrix $R = R_\omega R_\phi R_\kappa$ is estimated by least squares adjustment from the three conjugated normal vectors as:

$$\vec{n}_{i2} = R\vec{n}_{i1}$$

Theoretically one pair of normal vector is sufficient to calculate the values of ω, ϕ, κ. We use two pairs of normal vectors and computed the angular parameters with a least squares solution. A third planar roof wa also determined and used for check purposes. As all planar primitives are horizontal planes, the three components of normal vectors are very close to (0, 0, 1). We observed that with these values of normal vectors three angles are numerically very sensitive to the planes being almost parallel. Non-accurately derived planes and thus normal vectors lead to quite different angular parameters.

The translation matrix $T = \begin{bmatrix} T_X & T_Y & T_Z \end{bmatrix}^T$ between the corresponding planes is estimated from the conjugate plane centroids as:

$$T = \vec{m}_{i2} - R\vec{m}_{i1}$$

and

$$T_X = \frac{\sum_i^k \left(\overline{X}_{i2} - R\overline{X}_{i1}\right)}{k}$$

$$T_Y = \frac{\sum_i^k \left(\overline{Y}_{i2} - R\overline{Y}_{i1}\right)}{k}$$

$$T_Z = \frac{\sum_i^k \left(\overline{Z}_{i2} - R\overline{Z}_{i1}\right)}{k}$$

where *k* is the number of planes.

2.6 Assessment of the co-registration

The assessment of the co-registration of the lidar and photogrammetric data is performed in both the object space and the image space.

In the object space the differences of normal vectors $\Delta\beta = \left(\vec{n}_2 - R\vec{n}_1\right)$ and plane centroids $\Delta m = \left(\vec{m}_2 - R\vec{m}_1\right)$ are evaluated as part of the transformation solutions. In addition the results after the co-registration can be visualized to see if the planes are correctly overlap.

Further lidar derived roof shapes are first transformed to the photogrammetric DSM system and then are back-projected to the image space using the collinearity equations and the known interior and exterior orientation parameters of the images used to derived the photogrammetric DSM. The differences in the image coordinates between the projected lidar shapes and the image shapes can serve as another accuracy measure based on the image scale.

3. PRELIMINARY RESULTS

3.1 Data sets and reference systems

The study area in this work is the Keele Campus, York University in North York, Toronto. The DSM has a resolution of 0.78m. Its X and Y are in the NAD83 UTM coordinate system and its Z are orthometric heights. It has been derived from UltraCam digital aerial images of Campus taken in 2005 from a flying height of about 1660m. The lidar data were generated in 2009 from a flying height of about 2000m and have point density of about 3 points/sq m. Its X and Y are in the NAD83 UTM coordinate system and its Z are ellipsoidal heights.

3.2 Plane segmentation and fitting

The approach described in the methodology sections was applied to both DSM and Lidar data sets. In our test, three planes from both datasets were selected from extracted plane primitives and assigned together manually according to their correspondence. Experimentally, the maximum angle between two normal vectors was set as 20 degree. The quality of the derived planes was assessed based on the residual values (Table 1). We noticed that the lidar planes have been better derives as their residuals are about half the magnitude of the residuals resulted from the plane fitting to DSM planar clusters.

	Lidar planes (input data)		
	RMSE (m)	max residual (m)	min residual (m)
building 1	0.04	0.32	-0.31
building 2	0.05	0.25	-0.18
building 3	0.05	0.17	-0.22
	DSM planes (reference data)		
	RMSE (m)	max residual (m)	min residual (m)
building 1	0.12	0.49	-0.49
building 2	0.09	0.59	-0.33
building 3	0.14	0.48	-0.55

Table 1: Plane fitting residuals

The two normal vectors used to estimate dthe rotation matrix *R* derived from the coefficients of the first and third planes are:

N1 = [0.0006883403911591 -0.0004354097794264 1
0.0015068327611961 -0.0001548050411902 1];

N2 = [0.0010081032931316 -0.0002873558702306 1
0.0029169238856444 0.0003340093587079 1];

Each row in N1 represents a plane's normal vector components extracted from Lidar dataset while each row in N2 represents a plane's normal vector that extracted from DSM dataset. Figures 1 to 3 show the generated planes reprojected on to the aerial images. As we can see the DSM planar points fall within the building boundaries in the background image while the lidar planar points have a shift in both x and y components. This because the DSM data were generated from this aerial image hence the back-projection of DSM should fit the building boundaries in image. However, the lidar dataset are displaced due the fact that their elevations were ellipsoidal heights instead of orthometric heights as the DSM elevation. Therefore, the shifting in the image represents the radial displacement due to height differences.

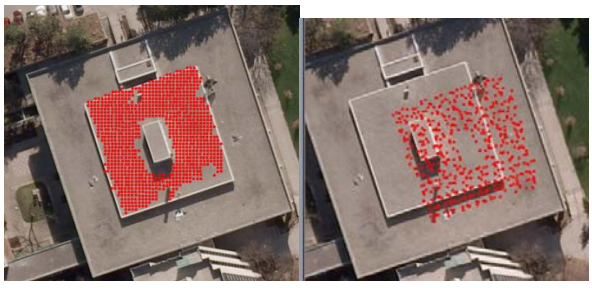

Figure 1. First pair of planes: DSM left and Lidar right.

3.3 Results of Transformation

The transformation matrix was calculated using the two pairs of normal vectors extracted from both DSM and Lidar data sets. Since DSM has been generated from the aerial images, it was

Figure 2. Second pair of planes: DSM left and Lidar right.

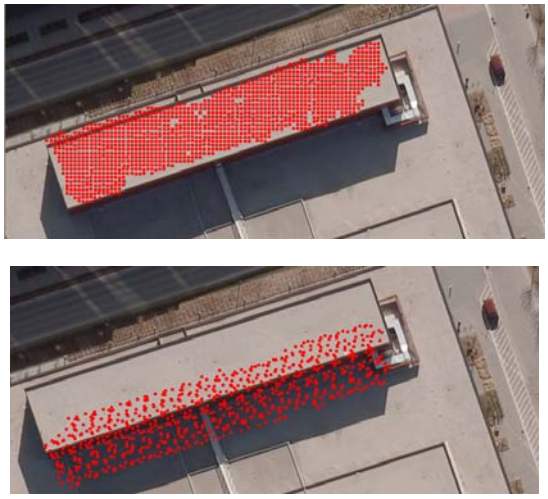

Figure 3. Third pair of planes: DSM top and Lidar bottom.

set as the reference system while lidar planes were set as input data as we are interested in detecting changes between photogrammetric and lidar data. Any spatial changes will be the mis-match between the re-projected lidar data on the images and the image data. The 3D mapping function that transforms the lidar planes to DSM coordinate system consist of the rotation matrix *R* and the translation vector *T*:

R = [0.999932876 -0.011554420593 0.00086034659755
0.011554161 0.999933201604 0.00030609268516
-0.000863826 -0.000296131556 0.9999995830 5541]

T = [0.54 0.77 38.18] (m).

The transformation was applied as follows. Firstly, the Lidar data are reduced to common centroid coordinate system where the 3D transformation is applied. Then they are transformed to object space using the centroid shifts to get the actual transformed lidar data in the DSM coordinates system. Afterwards using the interior and exterior parameters of the images the lidar point cloud is back-projected to corresponding image. The results are shown in Figure 4.

The rotation and translation residuals are given in Tables 2 and 3:

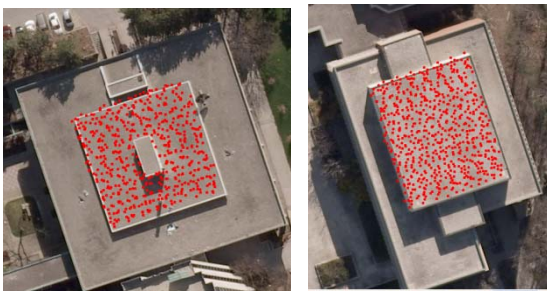

(a) (b)

(c)

Figure 4. Lidar planes after the transformation. (a), (b) and (c) represent the results of building 1, 2 and 3, respectively.

dn_X	dn_Y	dn_Z
0.001189	0.000452	-4.2E-08
0.001553	-0.00291	5.98E-07
0.002276	0.000802	-8.3E-07

Table 2: Normal vector residuals $\Delta\beta$ after rotation.

dX	dY	dZ
0.54	-0.38	0.07
0.24	-0.95	-0.01
-0.77	1.32	-0.05

Table 3: Shifts residuals Δm after translation (m).

4. CONCLUDING REMARKS

An approach has been presented for the co-registration of lidar and DSM point clouds captured from difference time epochs. The correspondence between the two different point clouds is established with the assistance of planar surfaces generated based on the 3D points. A region growing algorithm is applied to derive point clusters belonging to the same roof plane. The parameters of the planes best fit to the point cluster are calculated by least square adjustment. Each plane is represented by its normal vectors and gravity center. Then the correspondence between each plane in each data set was manually constructed. A 3D transformation consisting of a rotation matrix and a translation matrix is then derived based on the normal vector and gravity centres of correspondent planes. Afterward the lidar point cloud is mapped on the images for quality assessment and change detection. The results indicate that this method for aligning 3D point clouds surfaces is promising. Our future work will investigate the use the integration of planar, linear and point data for co-registering

pjhotogrammetric and lidar data. It will also address the quality of the extracted features and its impact of the transformation parameters. In addition methods for automatically establishing the correspondence and matching of the selected primitives will be investigated.

ACKNOWLEDGEMENTS

The financial support by the Natural Research Council of Canada (NSERC) and the Korean Land Spatialization Group (KLSG) is greatly appreciated. The authors are also grateful to FirstBaseSolutions and Optech Inc. for providing the DSM and lidar data respectively.

REFERENCES

Besl, P. J. and N. D. McKay, 1992. A Method for Registration of 3-D Shapes, *IEEE Transactions on Pattern Analysis and Machine Intelligence*, 14(2):239-256.

Chikomo F.O., J. P. Mills and S.L. Barr, 2007. Adaptive Building Model Reconstruction From Airborne Lidar and Optical Imagery. *RSPSoc Annual Conference. Newcastle upon Tyne*.

Dold, C. and Brenner, C., 2004. Automatic matching of terrestrial scan data as a basis for the generation of detailed 3D city models. *International Archives of Photogrammetry, Remote Sensing and Spatial Information Sciences*, Vol. XXXV, part B3, p. 1091 ff.

Habib, A., T. Schenk, 1999. New approach for matching surfaces from laser scanners and optical sensors, *The International Archives of Photogrammetry and Remote Sensing and Spatial Information Sciences*, 32(3W14):55-61.

Habib, A., M. Ghanma, and E. Mitishita, 2004. Co-registration of photogrammetric and LIDAR data: Methodology and case study. Revista Brasileira de Cartografia 56(1): 1-13.

Postolov, Y., A. Krupnik, and K. McIntosh, 1999. Registration of airborne laser data to surfaces generated by Photogrammetric means. *International Archives of Photogrammetry and Remote Sensing*, 32(3W14): 95-99.

Sampath, A., Jie Shan, 2006. Clustering based planar roof extraction from lidar data, *American Society for Photogrammetry and Remote Sensing Annual Conference*, Reno, Nevada, May 1-5.

Schenk, T., and B. Csathó, 2002. Fusion of lidar data and aerial imagery for a more complete surface description, *International Archives of Photogrammetry and Remote Sensing*, 34(3A):310–317.

Shan, J. and D. Lee, 2002. Generalization of building polygons extracted from IKONOS imagery. *International archives of Photogrammetry Remote Sensing and Spatial Information Sciences*, 34(4): 297-304.